INVESTIGATION OF CLOUD PROPERTIES AND ATMOSPHERIC STABILITY WITH MODIS

SEMI-ANNUAL REPORT FOR JAN-JUN 1996

Paul Menzel, Steve Ackerman, Chris Moeller, Liam Gumley, Kathy Strabala,
Richard Frey, Elaine Prins, Dan LaPorte and Mervyn Lynch
CIMSS at the University of Wisconsin
Contract NAS5-31367

ABSTRACT

The last half year was spent in preparing Version 1 software for delivery, and culminated in transfer of the Level 2 cloud mask production software to the SDST in April. A simulated MODIS test data set with good radiometric integrity was produced using MAS data for a clear ocean scene. ER-2 flight support and MAS data processing were provided by CIMSS personnel during the Apr-May 96 SUCCESS field campaign in Salina, Kansas. Improvements have been made in the absolute calibration of the MAS, including better characterization of the spectral response for all 50 channels. Plans were laid out for validating and testing the MODIS calibration techniques; these plans were further refined during a UW calibration meeting with MCST.

TASK OBJECTIVES

Software Development

Cloud mask, cloud top property and atmospheric profiles science production software continue to evolve. The software which generates the cloud mask product (MOD35) was delivered in April. The ancillary data processing software was delivered as production code in June. The remaining software packages will be delivered in third quarter 1996.

ATBD Evolution

The UW ATBDs will be revised to include information from the validation plan and the continuing MAS, AVHRR, HIRS, and GOES cloud investigations. Another version of the ATBDs will be drafted in third quarter 1996.

MODIS Infrared Calibration

Plans are being implemented for testing of the MODIS calibration schemes. These plans include testing the IR calibration ATBD with GOES data as well as MODIS vacuum test data.

WORK ACCOMPLISHED

MODIS Software Development

Several steps were taken toward completion of all V1 cloud and atmospheric properties production Level 2 and Level 3 software due second and third quarters of 1996. This progression included the delivery of the production software cloud mask (MOD35) in April and the ancillary data pre-processor in May to the SDST. An outline of the software development is provided below.

(1) In order to provide a source of ancillary data for the UW MODIS algorithms, software was developed to ingest and resample National Center for Environmental Prediction (NCEP) global analysis data to MODIS Level-1B granule resolution. Data samples were obtained from the NCEP anonymous FTP site at nic.fb4.noaa.gov for this purpose. The data products included

- Global Aviation Model, 1x1 degree, 0 and 12 UTC analysis, daily (GRIB format)
- Reynolds Optimum Interpolation SST, 1x1 degree, weekly (ASCII format)
- TOVS Total Ozone, 1x1 degree, daily (GRIB format)

The Global Aviation (AVN) Model was selected initially because it contained all the desired variables. A different model may be used in the future once we examine the algorithm impact of the AVN model data. The variables extracted were

- temperature (K)
  (1000, 925, 850, 700, 500, 400, 300, 250, 200, 150, 70, 50, 30, 20, 10 hPa)
- water vapor mixing ratio (g/kg)
  (1000, 925, 850, 700, 500, 400, 300 hPa)
- surface temperature (K)
- surface pressure reduced to mean sea level (hPa)
- precipitable water (kg/m^2)
- surface wind u component (m/s)
- surface wind v component (m/s)
- sea ice concentration (fraction)
- sea surface temperature (K)
- total ozone (Dobsons)

FORTRAN code was developed for the following tasks:

- convert GRIB global data to FORTRAN unformatted sequential (code from NCEP)
- convert FORTRAN unformatted sequential global data to HDF SDS
- interpolate HDF SDS global data to MODIS geolocation lat/lons

The FORTRAN tools and corresponding input and output data sets were delivered to SDST. The output data set (in HDF SDS format) will also be used by other MODIS

Atmosphere Group investigators who otherwise had no source for ancillary data at MODIS spatial resolution. Capabilities which will be added in the future include interpolation in time between input data sets, and quality control of the input data. An example of the UW MODIS ancillary data product is shown in Figure 1.

(2) All required MODIS tools available at the time of delivery were implemented in UW algorithm software. These included the MODIS Application Programmer Interface (MAPI) and the Science Data Processing (SDP) Toolkit.

(3) The Process Control File (PCF) was redesigned to allow access to the correct Version 1 input and output data sets.

(4) Improvements have been made to the cloud mask processing software since the Beta version. The software has been streamlined, documented and updated to produce a 48 bit cloud mask product. The Olson World Ecosystem Map has been incorporated to enable definition of more surface type processing paths, including deserts. A simple snow background test has been included, along with a thin cirrus test. Tests on single high resolution 250 m pixels have been added. NCEP ancillary data are now read as inputs. Clear radiance maps are now generated for the infrared window channel (11 micron, channel 31) and the four CO_2 channels (13.3 - 14.1, channels 32-36). The CO_2 channel clear radiance maps are created for input to the cloud top properties production software. The output cloud mask HDF file was updated to conform with file specifications. The file contains the results in the updated 48 bit cloud mask format.

(5) A fast algorithm for MODIS atmospheric temperature and moisture retrieval was implemented by Hal Woolf, UW-CIMSS. This is a regression-based statistical retrieval similar to those that have been used operationally on NOAA HIRS data for almost two decades. Preliminary timing estimates indicate that the algorithm (not including data I/O) is about one thousand times faster than the physical algorithm delivered for Beta. Work is progressing on preparing the new fast algorithm for V1 delivery.

(6) As there were no visualization tools available for MODIS HDF products, UW developed some in IDL. Procedures were developed for

- reading individual SDS's from HDF product files,
- displaying individual SDS's on a map projection using MODIS geolocation information,
- displaying images in multiple image frames to allow rapid frame switching and looping.

These tools will be made available to the MODIS Atmosphere Group via the World Wide Web at http://cimss.ssec.wisc.edu/~gumley/index.html. See Figure 1 for an example of the imagery created by the UW IDL tools.

(7) GSFC provided a license for the IMSL math library, which has been installed on the UW Science Computing Facility SGI. IMSL will be initially investigated for a means of resampling 1x1 degree global gridded data to MODIS spatial resolution.

(8) A set of simulated Level 3 MODIS global monthly mean cloud product files have been generated. CHAPS (Collocated HIRS and AVHRR ProductS) single FOV data were used as input to software which produced representative monthly values stored in HDF output files. CHAPS data include cloud products generated from HIRS/2 pixel radiances using the CO_2-slicing algorithm. The simulated products consist of minimum collocated AVHRR temperature, cloud top pressure, effective emissivity, frequency of transmissive clouds, and frequency of high clouds for the month of July 1994. The monthly means and frequencies were computed at 0.5 degree resolution on both equal-angle and equal-area grids. An image of the high cloud frequency product on the equal-angle grid is shown in Figure 2. Since the full CHAPS algorithm was applied only for ocean areas, the quality is highest there. Also, the original HIRS/2 data was sub-sampled by a factor of 5 in polar regions.

MAS Cloud Mask Code Converted to non-McIDAS Format

An updated and revised version of the fifty channel MAS cloud mask code has been made available. The new version does not require the McIDAS software package or input data in McIDAS formats. MAS radiance and earth location data from January 13, 1995 were converted from McIDAS Digital Area format into simple binary direct access files. The software was revised accordingly and updated to accommodate recent changes in the cloud mask algorithm. The code was transferred to GSFC for use by the cloud retrieval group.

MODIS IR Calibration

On 14 March 1996, Dan Knowles and Gerry Godden visited UW to discuss the MODIS IR calibration algorithm. Several issues were discussed and the following key points emerged.

(1) Smooth changes in the calibration equation are absolutely necessary so that they reflect what is really happening in the MODIS instrument. This will most likely require averaging blackbody views (keeping 1/f noise in mind). The calibration of adjacent granules must be related.

(2) A linear form of the quadratic calibration equations will be the automatic default for those spectral bands with negligible non-linearity.

(3) The form of the calibration equation R = f(V, V2) is largely equivalent to V = f(R, R2).

(4) Changes of the calibration algorithm as a function of scan angle are adequately determined with linear rather than quadratic interpolation.

(5) Anticipated striping in the ten detectors for one spectral band images will require considerable attention. Some destriping approaches need to be investigated.

The UW has also reviewed the calibration ATBD. The algebra in the ATBD has been subjected to a detailed check and found to be correct. With the assumption that the detector non-linear coefficients (α) can be small, we have explored the behavior of the expressions for (i) the calibration coefficients m, L_0, and the product quantity m L_0, and (ii) the associated quantities dm/d(α), d L_0 /d(α) and d(m L_0)/d(α) in the limiting case of $\alpha \sim 0$.

The independent evaluation of the performance and stability of the IR calibration procedure as described in the ATBD requires that a sample test data set be assembled from the MODIS EM test data. To achieve this end, with the assistance of the MCST, UW has sought for some months the key pieces of data but unfortunately has not succeeded in acquiring it to date. Some key items of information are missing and some appear to require scaling factors for them to assume physically meaningful values. UW has only addressed the calibration for the case of 'charge integration off'. Plans are to use the EM data set to generate the calibration coefficients and other quantities listed in (i) and (ii) and to establish the stability and uniqueness of the solutions using real rather than simulated data.

UW continues to have concerns that the detector performances, as judged by the EM test data, show widely varying non-linear responses with a significant number of detectors appearing to not conform with a physically acceptable behavior.

HIRS Cloud Climatology

The seven year HIRS CO2 slicing cloud climatology is being examined for trends in light cirrus in different parts of the world. The overall trend shows an increase in light cirrus over the seven year period. One reason for this increase may be the growth in the number of upper tropospheric commercial airline traffic around the world. A steeper increase in light cirrus over heavy air traffic regions versus those of low traffic regions may support this theory.

MAS SCAR-B Fire Scene Calibration

A linear calibration was finalized for the MAS 1.6 and 2.1 micron channels and delivered to GSFC (Yoram Kaufman's group). Emissivity of source blackbody in the near infrared spectral region was assumed to be one. The calibration does not include an adjustment to the calibration slope based on instrument operating temperature. Previous work at GSFC has shown near infrared MAS channel calibration to be a function of instrument operating temperature. This adjustment will be generated at GSFC. The calibration is valid for MAS SCAR-B data and will be used at GSFC to estimate fire temperature from MAS near infrared data.

GOES Biomass Burning Program

The SCAR-B data set and other ancillary case studies throughout the Western Hemisphere are being used to refine the GOES-8 ABBA and aerosol detection algorithms. An overview of the preliminary SCAR-B ABBA fire results and aerosol extent and transport regimes was presented at the SCAR-B workshop and data analysis meeting at GSFC on 20-22 March. Possible areas of scientific collaborations between US and Brazilian investigators were discussed. As part of GOES-8 ABBA validation efforts, UW-Madison is collaborating with the USFS to use ground truth data collected by the USFS during SCAR-B to verify GOES-8 ABBA fire location and size estimates. A related SCAR-B activity involves a collaborative effort with Jackie Kendall (GSFC) and Chris Elvidge (NGDC) to compare active fire products derived from NOAA, GOES, and DMSP for two of the peak burning days during SCAR-B (22 and 24 August 1995). This intercomparison study is being led by Jackie Kendall at GSFC. A preliminary review of the intercomparison study was presented by Ms. Kendall in the BIBEX session at the XXI General Assembly of the European Geophysical Society in The Hague, Netherlands on 8 May 1996.

In related activities, case studies of GOES-8 fire monitoring capabilities throughout the Western Hemisphere are demonstrating the unique ability of the GOES-8 to serve as an early warning fire detection mechanism for identifying and monitoring diurnal variations in wildfire size and intensity. GOES-8 case studies collected in 1995 and 1996 include wildfires in Central America; grassland fires in Texas, Oklahoma, and Nebraska; the fire on Long Island in New York; and numerous examples of wildfires in the temperate forests of the western United States and the boreal forests in Canada.

GOES-8 fire detection capabilities and applications of the GOES-8 ABBA throughout the Western Hemisphere were presented at the 22nd Conference on Agricultural and Forest Meteorology with Symposium on Fire and Forest Meteorology in Atlanta, GA in January 1996. An overview of the UW-Madison GOES ABBA fire detection and aerosol monitoring program in South America was presented at the Seventh Symposium on Global Change Studies which was also held in Atlanta, GA. An oral presentation on monitoring biomass burning and aerosol loading and transport utilizing multispectral GOES-8 data was given in the BIBEX session at the XXI General Assembly of the European Geophysical Society in The Hague, Netherlands on 7 May 1996. In conjunction with the BIBEX session, Elaine Prins attended the BIBEX Steering Committee meeting which included a discussion of the results of the IGBP-DIS Global Fire Monitoring Workshop in Italy in October 1995. The conference and BIBEX meeting served as a venue for discussions concerning future international global fire monitoring efforts which may include fire products derived from NOAA AVHRR, DMSP, MODIS, and geostationary platforms.

This work is supported by separate NASA and NOAA contracts.

Satellite Conference Presentations

The MAS 50 channel cloud mask algorithm and MAS, GOES-8, HIS, and AVHRR data split window studies were presented as posters at the 8th Conference on Satellite Meteorology and Oceanography in January. Cloud masks for varying MAS scenes were produced and displayed as preparation for the MODIS day-1 cloud mask product. Differences between MAS, HIS, GOES-8 and AVHRR T11-T12 were investigated and displayed in regions where negative values were found.

Participation in the SUCCESS Field Program

University of Wisconsin personnel (Ackerman, Moeller, Strabala, Gumley) supported MAS instrument performance, data product archival, science product generation, case study investigation, and ER-2 mission planning during the campaign. An SGI workstation was generously provided by GSFC to facilitate processing of MAS raw data and production of MAS archive products for the SUCCESS Data Exchange Archive.

The MAS instrument flew 18 missions on the ER-2 aircraft during the SUCCESS field experiment conducted out of Salina, KS from April 8 to May 10, 1996 and continued from Moffett Field, CA from May 10-15. The MAS data set is of excellent quality, including observations of persistent and non-persistent aircraft contrails, cirrus clouds, mountain lee wave clouds, and convective cloud. MAS brightness temperature and quick look imagery products were submitted to the SUCCESS archive for each flight. Cloud top properties were generated in the field for selected cases. Many interesting observations were collected during SUCCESS. In particular, cirrus cloud and contrail radiative properties were differentiated using plots of 8-11 micron brightness temperature versus 11-12 micron brightness.

Figure 3 plots a short time series of Cloud Lidar System (CLS) derived cloud tops and bottoms and infrared observations from the MAS. The left hand axis is the CLS derived cloud boundary in kilometers, a quick look product produced in the field by GSFC (J. Spinhirne). The blue circles and red squares represent the boundaries of the first cloud detected. The first cloud is detected just prior to 1955 UTC and is approximately 1000 meters thick at 1957 UTC. The cloud between approximately 5 and 4 km is present during most of this time interval. Shortly after 1960 UTC three layers of cloud are detected by the lidar. The upper most clouds are between approximately 9 and 7 km. The green diamonds and magenta triangles denote the second cloud detected from the ER-2 altitude and retrieved by the lidar algorithm. The solid black circles and filled gray squares are the third layer detected by the lidar (the lidar algorithm detects a maximum of 5 cloud layers). The blue circles are a surface return signal. The surface signal (e.g. approximately 1965 UTC) is not seen in optically thick clouds.

The right hand y-axis denotes the observed brightness temperature differences observed by the MAS. The dotted red line is the 11 micron minus 12 micron temperature difference and the dotted green line is the BT8-BT11 difference. Differences between these channels are used to detect cloud and determine phase of the water. Negative differences in BT8-BT11 usually occur in clear sky conditions. The bottom of Figure 3 lists the approximate locations of HIS observations in terms of HIS record number. They are color coded with Figure 4 which displays HIS observed radiances converted to brightness temperatures as a function of wavenumber (inverse cm -- bottom axis) and wavelength (micron -- top axis). HIS spectra 515 was measured at 1932 UTC and is of a clear sky scene as shown by the lidar observations. Spectral signatures of many gases are evident in these measured radiation spectra. At 1934 UTC HIS spectra 526 displays a signature associated with ice cloud conditions. This is consistent with the large BT8-BT11 differences observed by the MAS. HIS spectra 534 (1936 UTC) displays an approximately 20 degree K temperature difference between 10 and 12 microns. MAS brightness temperature differences are also large at this time and correspond with BT11-BT12 > BT8-BT11, suggesting this is liquid water cloud. HIS spectra 540 (1937 UTC) is similar to that of 526 and is taken over a multi-level cloud scene as suggested by the lidar data. Here MAS BT8-BT11 > BT11-BT12; indicating ice cloud. HIS spectra 546 (1938 UTC) was taken over a two cloud layer where one of these clouds was thick (as indicated by the absence of a CLS surface return). MAS BT8-BT11 and BT11-BT12 are both close to zero at this time, an indication of an opaque cloud.

In situ measurements from the DC-8 aircraft show that contrail particles are typically much smaller (< 20 microns) than naturally occurring cirrus particles (~ 50 microns). Scenes of vigorous convection showed negative 11-12 micron brightness temperature differences in the HIS data set. This occurrence, while previously observed by GOES and other instruments, had never before been validated by the excellently calibrated HIS observations. Missions over the ARM CART site included thick to thin cloud cover as well as clear scenes for radiative comparisons between ground based and aircraft based instrumentation. Many of these data sets will support MODIS cloud mask algorithm development. The MAS thin cirrus detection channel (1.88 microns) demonstrated excellent skill at depicting thin cirrus cloud and contrails in the upper troposphere.

Japanese Satellite Workshop

A Advanced Earth Observing Satellite - II (ADEOS-II) Global Imager/Advanced Microwave Sounding Radiometer (GLI/AMSR) Workshop was held in Hakone, Japan, 26-28 June, for initializing PI team activities of the GLI&AMSR project for the ADEOS II. The MODIS Atmosphere group was represented by Drs. King, Tsay (Goddard) and Ackerman (University of Wisconsin). The Goddard/UW team participation in ADEOS-II is to coordinate activities to transfer the MODIS atmosphere algorithms to the GLI Atmosphere Science Group lead by Dr. T. Nakajima. This meeting initiated these activities. The schedule of the research activities is as follows:

Start of algorithm research (Oct. 96)

Delivery Evaluation data sets for Selection of standard algorithm (Dec. 96)
2nd GLI/AMSR Workshop and detailed presentation of PIs algorithms (June. 97)
Selection of standard algorithm (Oct. 97)
Starts of algorithm development with Tool kit (Oct. 97)
Final decision of standard algorithm (Sep. 98)

DATA ANALYSIS

Simulation of MODIS Level-1B Data using the MODIS Airborne Simulator

In support of MODIS algorithm development at UW-Madison, MODIS Level-1B data was simulated using data acquired by the MODIS Airborne Simulator. The motivation for this effort was the need for a locally developed data set with good radiometric integrity and realistic scene variation. Goals of this effort include:

- approximating the MODIS bands spectrally as much as possible, with the available MAS bands,
- using real data where possible, and modeled data only where absolutely necessary,
- approximating the co-registration of MODIS bands (but not the spatial resolution),
- creating output data (Level-1B and geolocation) in HDF SDS format.

These goals have been met in Version 1.0 of the simulation for the simplest kind of MAS scene: open ocean with cloud-free skies. No limb or atmospheric corrections were applied. The MAS data were acquired on 16 January 1995 over the Gulf of Mexico during the OTIS experiment. The original unresampled MAS data contained 4000 scanlines, starting at 1555 UTC and ending at 1606 UTC. The direction of flight was approximately due east.

The MAS pixels (50 meter IFOV at nadir) were resampled to coarser spatial resolution to mimic the way that MODIS 250 meter pixels are registered to MODIS 500 meter and 1000 meter pixels. Here the objective was to mimic the MODIS relative band-to-band registration, ***not*** the absolute spatial resolution of MODIS. Put simply, the MAS 50 meter IFOV (at nadir) pixel was treated as being equivalent to the MODIS 250 meter pixel, and the MAS 50 meter pixels were sampled using weighting functions to create the relative equivalent of MODIS 500 meter and 1000 meter bands. In order to remove a 33% along track oversampling in the full resolution MAS data, every other MAS scanline was removed.

The MAS bands selected to simulate MODIS bands are shown in Table 1. MAS spectral responses were compared to MODIS spectral responses to find the best spectral agreement. 'Good' or 'OK' matches were found for 25 of the 36 MODIS bands. 'Good' refers to matches where a large portion of the MAS band and corresponding MODIS band spectral responses overlapped. 'OK' refers to matches where some spectral response overlap was found, and the MAS and MODIS bands were in similar absorption regions of

the spectrum. The remaining 10 MODIS bands were simulated using either the radiance from the closest (in wavelength) MODIS band for visible/near-IR bands, or a forward model calculation for IR bands. MODIS bands 27, 28, and 30 were simulated using a locally developed fast IR transmittance model. Temperature and moisture profile data for input to the fast model were obtained from a CLASS sonde launched at 1505 UTC on 16 January 1995 by the R.V. Pelican, which was located approximately at the center of the MAS scene in support of the OTIS experiment. The ocean surface was assumed to be at a uniform surface temperature of 298 K with unit emissivity. Scan angle effects were included in the simulation. A sample of the MODIS simulation of bands 28-36 by MAS data is provided in Figure 5.

The simulated MODIS Level-1B data were stored in HDF3.3r4 SDS form, using exactly the same variable and attribute names as were used in the MODIS Level-1B simulated data sets produced by SDST for the MODIS Software Beta delivery in October 1995. In the UW-produced data files, the global attributes 'CoreMetadata' and 'ProductMetadata' were not included. All units and scaling factors are identical to those used in the SDST produced data sets.

MAS Infrared Calibration

MAS spectral response has been characterized for all 50 MAS bands using July 1995 grating monochromator laboratory measurements. Central wavenumber and monochromaticity coefficients have been computed for all IR channels and made available to the MAS GSFC DAAC. Before delivery, the post processed spectral response data were compared to additional spectral measurements made in October 1995. A shift (~.05 micron) in Port 3 (SWIR) spectral response was noted. Port 4 showed good agreement. The spectral shift may be due to weakness in the dewar mounting of Port 3. This is under investigation at Ames Research Center (ARC). With a fully operational spectral calibration facility at ARC, spectral response of MAS bands will be characterized regularly; typically before field campaigns and after MAS hardware maintenance/modifications. As such, updated MAS spectral bandpass data will be available on a much improved temporal basis, resulting in improved absolute calibration of MAS.

In order to gain a better understanding of the channel spectral response functions, a series of spectral calibrations are being performed on the MAS using both a grating monochromator and a BOMEM MB100 Interferometer as the spectral calibration sources (Figure 6).

While the grating monochromator is the more traditional approach to make a spectral calibration, it has the disadvantage of measuring only one spectral interval at a time and not completely filling both the field of view and the aperture at the same time (Figure 7). In addition, since it is a sequential and time consuming measurement for 50 channels, it is not practical to measure each spectral band over a complete enough spectral range to check for unwanted or out of band spectral response.

The FTS approach is able to completely fill the field of view and cover the full spectral range of ports 2, 3, and 4 at much higher spectral resolution. The spectral resolution ($1cm^{-1}$) is high enough that measurements can be taken, on most channels, "through" the water vapor and CO_2 absorption of the laboratory atmosphere (Figure 8). The spectral reporting accuracy between the two methods is very good as shown in the comparison the position of the CO_2 features in channel 49 in Figure 9. A comparison of the MAS spectral response function measured with the two approaches is seen in Figure 10; channel 31 exhibits very good agreement but channel 42 results do not compare as well. Out of band response in channels 38, 39, 40, and 41 (Figure 11) was discovered by the interferometer where each channel was measured over the full spectral range of the interferometer (2.5 to 25μm) .

One additional step needs to be taken before the interferometer method is sufficiently proven to be the "standard" measurement method. The radiance uniformity of the interferometer output needs to be improved and the size needs to be enlarged slightly to fully cover the field of view of the MAS. Plans are in place to accomplish these changes this fall.

MAS blackbody effective emissivity estimates have been completed for the MAS infrared bands 26-50 (Figure 12) and delivered to the GSFC DAAC for incorporation into MAS Level 1B processing. The data analysis included effects of atmospheric attenuation (external source to instrument detector and onboard blackbody source to instrument detector) and non-unit source emissivity in the ambient laboratory measurement conditions. Strong absorption in CO_2 and H_2O sensitive channels was removed by smoothing the effective emissivity estimates (as a function of wavelength) with regression. The final effective emissivity estimates generally agree with the spectral shape of direct reflectance measurements (collected Feb 1996) of the MAS blackbodies.

Using the effective emissivity estimates in the MAS calibration, a comparison was made between MAS and HIS collocated data from January 13, 1995. Data scenes included thick cold cloud and clear warm water. The MAS-HIS LWIR biases using both unit and non-unit effective emissivity calibration are compared in Table 2. Non-unit effective emissivity calibration greatly reduces the biases to within uncertainty of laboratory instrument performance characterization. The biases also show fairly good spectral independence with the exception of channel 50, which is sensitive to CO_2 absorption and spectral response measurement error. When MAS-HIS brightness temperature differences are plotted for the data of Jan 13 (Figure 13), the use of effective emissivity calibration essentially eliminates bias dependence on scene temperature. These results are very encouraging. Further characterization of the MAS instrument operating temperature (a source of reflected radiance) remains. New MAS laboratory measurements of a well calibrated external source will be made. Additional comparisons between MAS and HIS using other Jan 1995 data sets and the recently acquired SUCCESS data set will be evaluated for MAS absolute calibration temporal consistency.

A paper summarizing these results has been accepted for oral presentation at the SPIE annual meeting in August 1996.

PAPERS

Moeller, C. C., O. K. Huh, W. P. Menzel, and H. H. Roberts, 1996: The use of aircraft-borne MAS data for mapping sediment transport along the Louisiana coast. Presented at the 2nd International Airborne Remote Sensing Conference, June 24-28, San Francisco, CA, ERIM, vol II, pp. 673-682.

Gumley, L. E., P. F. Van Delst, and C. C. Moeller, 1996: Satellite and airborne IR sensor validation by an airborne interferometer. Presented at the 2nd International Airborne Remote Sensing Conference, June 24-28, San Francisco, CA, ERIM, vol II, pp. 262-271.

Moeller, C. C., S. A. Ackerman, K. I. Strabala, W. P. Menzel, and W. L. Smith, 1996: Negative 11 micron minus 12 micron brightness temperature differences: a second look. Presented at the Eighth Conference on Satellite Meteorology and Oceanography, Jan. 28 - Feb. 2, Atlanta, GA, AMS, pp 313-316.

Ackerman, S. A., K. I. Strabala, R. A. Frey, C. C. Moeller and W. P. Menzel, 1996: Cloud Mask for the MODIS Airborne Simulator (MAS): Preparation for MODIS. Presented at the Eighth Conference on Satellite Meteorology and Oceanography, Jan. 28 - Feb. 2, Atlanta, GA, AMS, pp 317-320.

Ackerman, S. A, 1996a: Global satellite observations of negative brightness temperature differences between 11 and 6.7 microns. Accepted with revisions by J. of Atmos. Science.

Ackerman, S. A., 1996b: Remote sensing aerosols from satellites using infrared observations. Accepted to the Journal of Geophysical Research with minor revisions.

Bywaters, K.W., and E.M. Prins, 1996: An interactive WWW tool for coupling satellite and meteorological data in real time. Presented at the 12th Conference on Interactive Information and Processing Systems for Meteorology, Oceanography and Hydrology, Jan. 28 - Feb. 2, Atlanta, GA, AMS, pp 382-384.

King, M. D., W. P. Menzel, P. S. Grant, J. S. Myers, G. T. Arnold, S. Platnick, L. E. Gumley, S. Tsay, C. C. Moeller, M. Fitzgerald, K. S. Brown, and F. Osterwisch, 1996: Airborne scanning spectrometer for remote sensing of cloud, aerosol, water vapor and surface properties. Jour. Atmos. and Oceanic Tech., 13, 777-794.

Prins, E.M., and W.P. Menzel, 1996a: Monitoring fire activity in the western hemisphere with the new generation of geostationary satellites. Presented at the 22nd Conference on Agricultural and Forest Meteorology with Symposium on Fire and Forest Meteorology, Jan. 28 - Feb. 2, Atlanta, GA, AMS, pp 272-275.

Prins, E.M., and W.P. Menzel, 1996: Monitoring biomass burning and aerosol loading and transport from a geostationary satellite perspective. Presented at the Seventh Symposium on Global Change Studies, Atlanta, GA, Jan.28 - Feb.2, 1996, pp. 160-166.

Smith, W. L., R. O. Knuteson, H. E. Revercomb, W. Feltz, H. B. Howell, W. P. Menzel, N. Nalli, O. Brown, J. Brown, P. Minnett, and W. McKeown, 1996: Observations of the infrared radiative properties of the ocean - Implications for the measurement of sea surface temperature via satellite remote sensing. Bull. Amer. Meteor. Soc., 77, 41-50

MEETINGS

Paul Menzel, Chris Moeller, Elaine Prins and Kathy Strabala were presenters at the Eighth Conference on Satellite Meteorology and Oceanography, held Jan 28 - Feb 2 in Atlanta, Georgia.

Steve Ackerman attended a SUCCESS planning meeting to finalize plans for the experiment and to review and prioritize the mission and flight plans in light of meteorological expectations and available resources, 14-16 February at NASA Langley Research Center.

Kathy Strabala attended the Science Advisory Panel meeting at GSFC 27-28 February.

The UW hosted the follow-up MODIS IR calibration audit meeting in Madison on 13-14 March 1996.

Elaine Prins attended the SCAR-B workshop and preliminary data analysis meeting at GSFC on 21-22 March and presented an overview of UW-Madison SCAR-B GOES ABBA and aerosol monitoring activities.

Dan LaPorte assisted Ames Research Center in spectral calibration of the MAS in March.

Steve Ackerman attended an Aerosol Remote Sensing Workshop on 15-19 April sponsored by NASA/EOS in Washington, D.C.

Steve Ackerman, Chris Moeller, Liam Gumley and Kathy Strabala participated in the SUCCESS field experiment based in Salina, Kansas in April and May.

Paul Menzel and Dan LaPorte attended the MODIS Calibration Working Group Meeting at GSFC on April 30.

Kathy Strabala attended the MODIS Programmers Forum Meeting at GSFC on April 30.

Paul Menzel, Steve Ackerman, Dan LaPorte, Merv Lynch and Kathy Strabala attended the MODIS Science Team Meeting at GSFC on May 1-3.

Elaine Prins attended the 21st General Assembly of the European Geophysical Society in The Hague, Netherlands on 6-10 May 1996 and gave an oral presentation on "Monitoring biomass burning and aerosol loading and transport utilizing multispectral GOES-8 data" in the Biomass Burning Experiment (BIBEX) and Related Topics session. In conjunction with the BIBEX session she also attended the BIBEX Steering Committee meeting on 8 May.

Chris Moeller and Liam Gumley presented papers at the 2nd International Airborne Remote Sensing Conference, held June 24-28 in San Francisco.

Steve Ackerman attended the ADEOS-II GLI/AMSR Workshop on 26-28 June in Hakone, Japan.

Table 1: MAS and MODIS Spectral Band Equivalence

MAS	MODIS	$\bullet_{MODIS}$	Comments
2	1	0.64	OK match, MAS longer λ, small absorption
7	2	0.86	OK match, MAS longer λ, MODIS more absorption
1	3	0.47	No MAS equivalent, use MAS λ 0.55, minimal absorption in both
1	4	0.56	Good match, MAS shorter λ, minimal absorption
10	5	1.24	No MAS equivalent, use MAS λ 1.65, small absorption in both
10	6	1.64	OK match, MAS shorter λ, small absorption
21	7	2.13	OK match, MAS longer λ, MODIS broader, absorption in both
1	8	0.41	No MAS equivalent, use MAS λ 0.55, minimal absorption in both
1	9	0.44	No MAS equivalent, use MAS λ 0.55, minimal absorption in both
1	10	0.48	No MAS equivalent, use MAS λ 0.55, minimal absorption in both
1	11	0.53	OK match, MAS broader, MAS longer λ, minimal absorption
1	12	0.55	Good match, MAS shorter λ, minimal absorption
2	13	0.66	OK match, MAS broader and shorter λ, MAS more absorption
2	14	0.67	OK match, MAS broader and shorter λ, MAS more absorption
4	15	0.74	OK match, MAS broader and shorter λ, MAS more absorption
7	16	0.86	Good match, MAS broader, MAS more absorption
8	17	0.90	Good match, significant absorption in both
9	18	0.93	OK match, MAS broader, significant absorption in both
9	19	0.94	OK match, MODIS broader, significant absorption in both
31	20	3.75	Good Match
32	21,22	3.95	OK match, MAS shorter λ, no spectral features
33	23	4.05	OK match, MAS more absorption
36	24	4.46	OK match, MODIS more absorption
36	25	4.51	Good Match, MAS has twice the bandwidth
15	26	1.38	No MAS equivalent, use MAS λ 1.88
-	27	6.7	No MAS counterpart - simulated using MODIS fast model
-	28	7.3	No MAS counterpart - simulated using MODIS fast model
42	29	8.55	Good Match
-	30	9.73	No MAS equivalent, simulated using MODIS fast model
45	31	11.0	Good Match
46	32	12.0	Good Match
48	33	13.3	OK match, MODIS more absorption
49	34	13.6	OK match, MAS more absorption
49,50	35	13.9	No MAS equivalent, use average of MAS bands 49 and 50
50	36	14.2	OK match

Table 2. MAS-HIS brightness temperature biases for MAS LWIR channels using MAS unit and non-unit effective emissivity calibration for the data of January 13, 1995. MAS data for channels 48 and 49 were not useful due to inflight instrument system problems.

MAS channel	MAS central wavelength μm (wavenumber cm^{-1})	MAS-HIS Bias (Unit emis. cal.) °C	MAS-HIS Bias (Non-unit emis. cal.) °C
42	8.59 (1164.3)	-3.78	-0.47
43	9.77 (1023.4)	-4.30	-0.74
44	10.54 (949.2)	-3.85	-0.64
45	11.01 (908.1)	-3.73	-0.50
46	11.97 (835.7)	-3.30	-0.13
47	12.85 (778.1)	-3.40	-0.23
50	14.19 (704.9)	-3.23	1.10

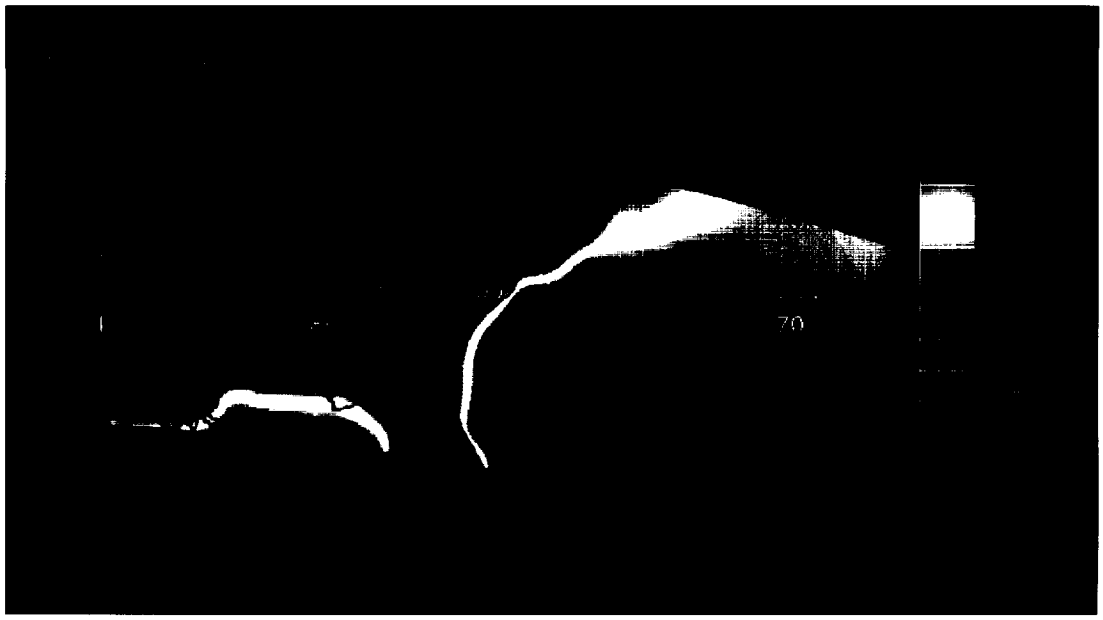

Figure 1. UW MODIS ancillary data product.

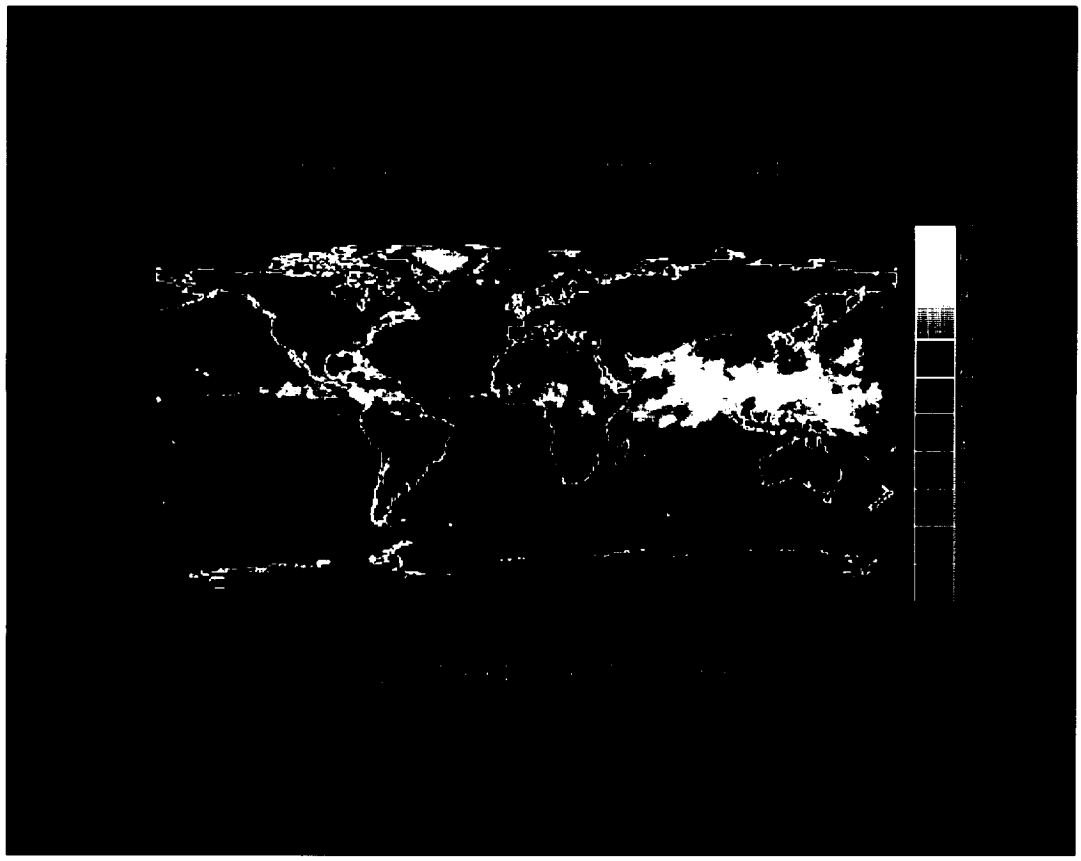

Figure 2. Example of a simulated Level 3 MODIS product created from CHAPS data.

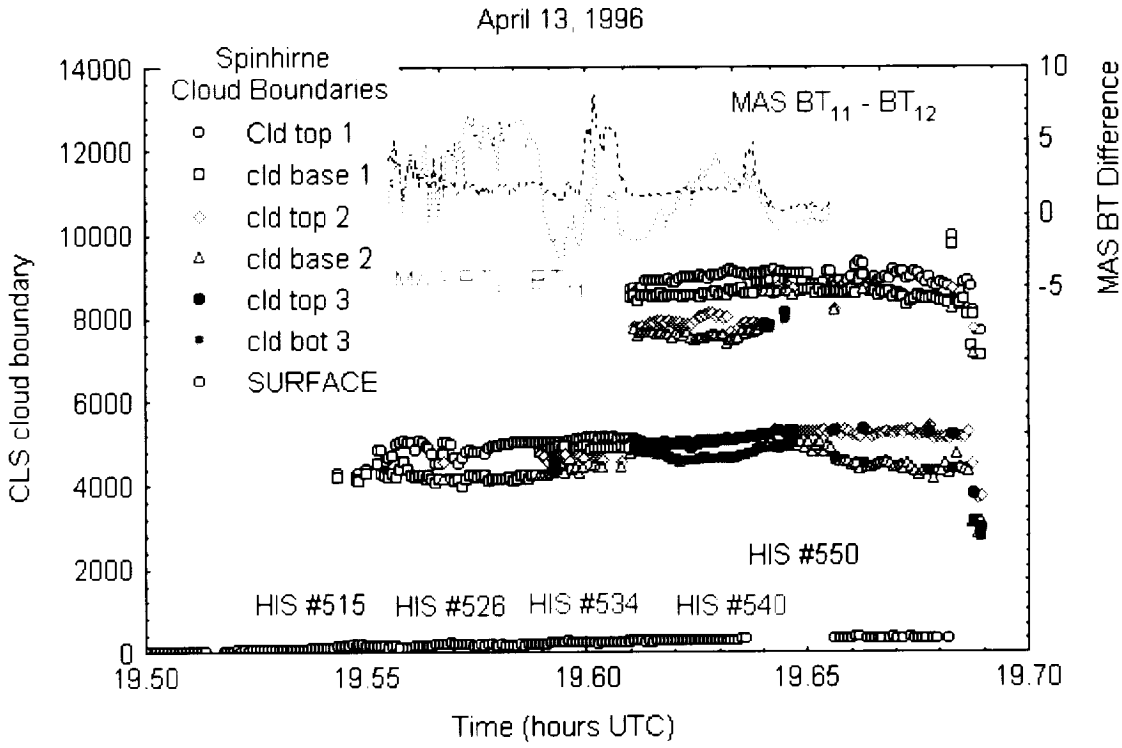

Figure 3. Combined MODIS Airborne Simulator (MAS) brightness temperature differences, High-Resolution Interferometer Sounder (HIS) record numbers and Cloud Lidar System (CLS) observations from 13 April 1996.

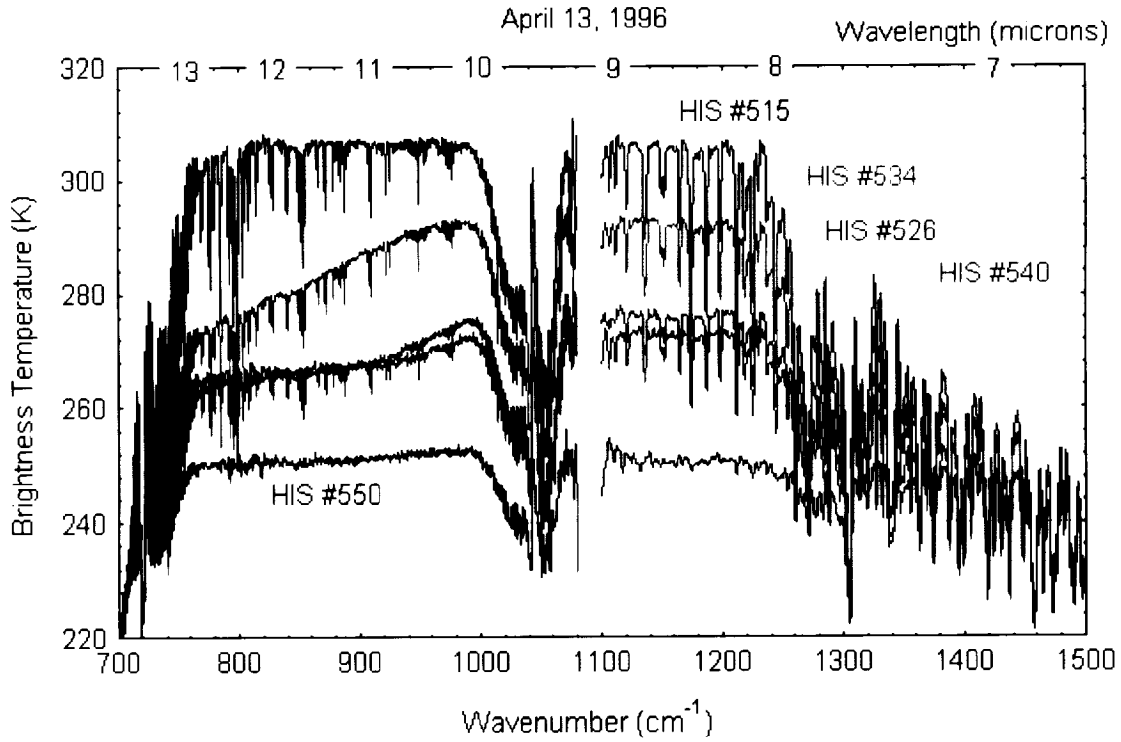

Figure 4. HIS observations for record numbers shown in Figure 3.

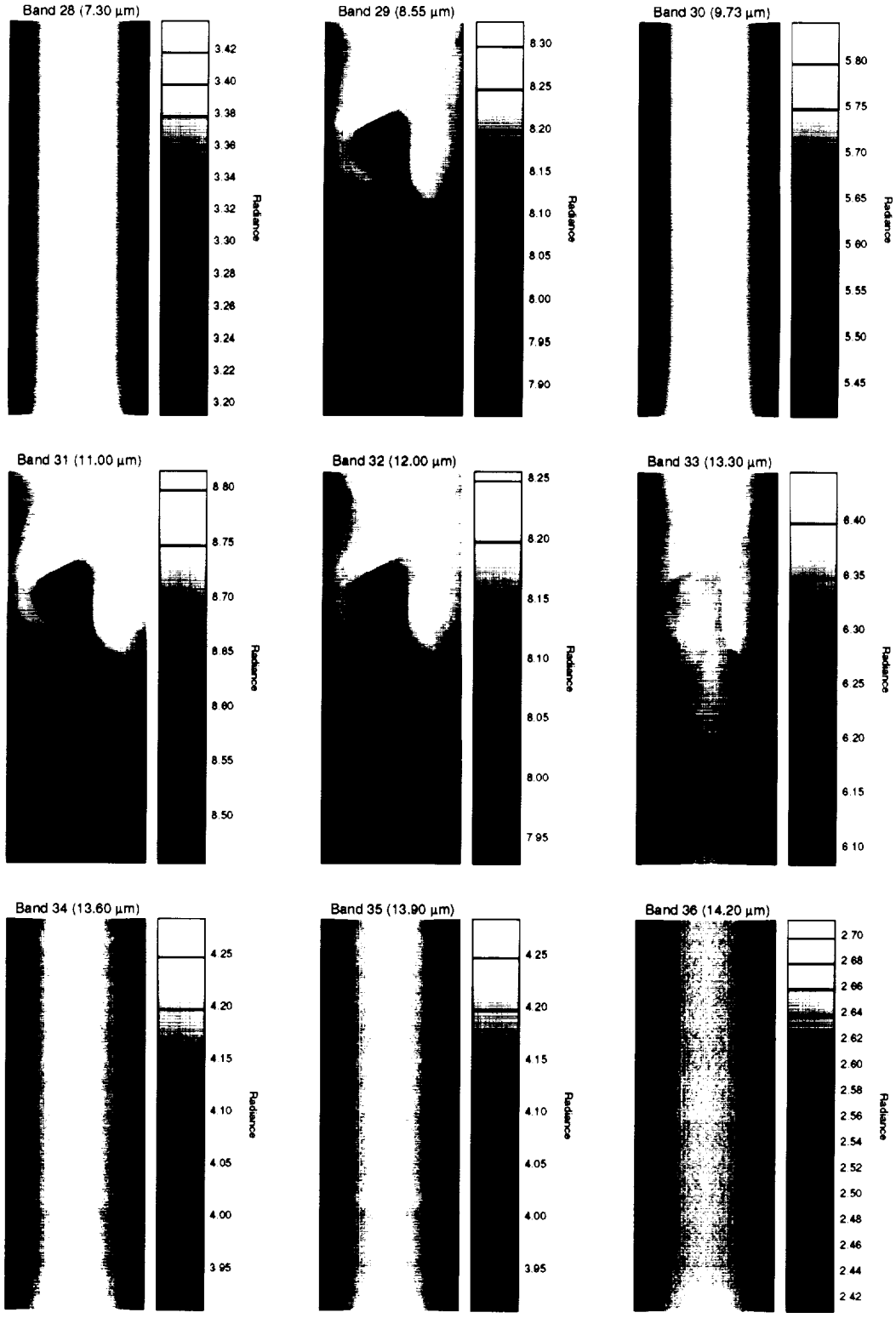

Figure 5. MODIS bands simulated by MAS

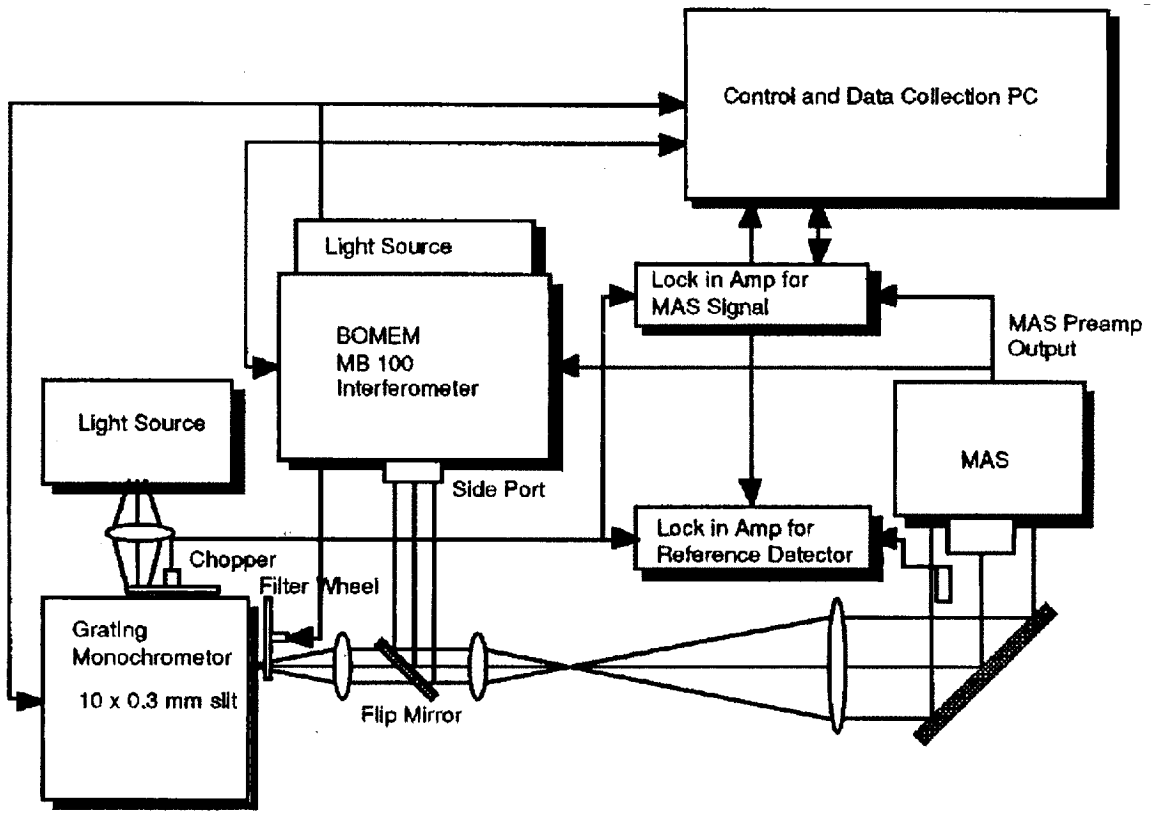

Figure 6. The schematic of the AMES spectral calibration facility including both grating monochromator and interferometer calibration sources.

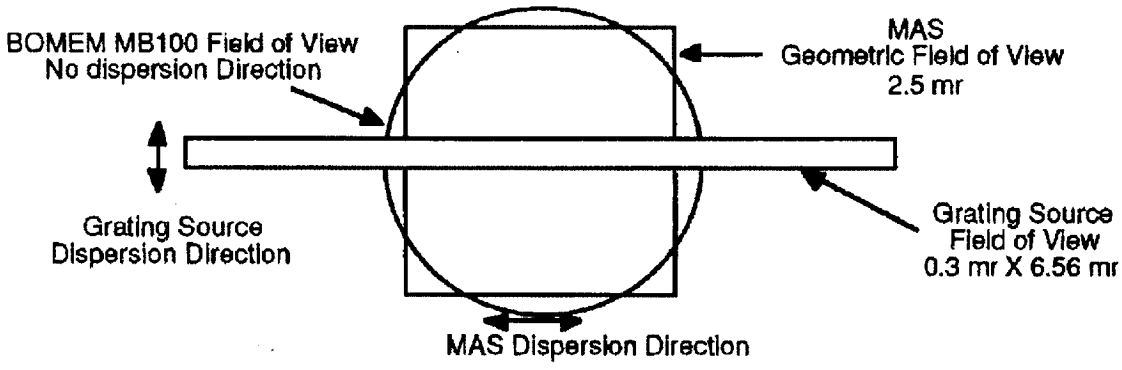

Figure 7. Dimensions of the MAS field of view and the relationship of the grating and interferometer spectral calibration sources.

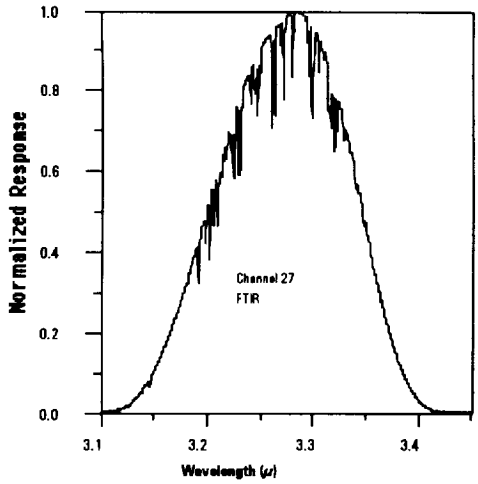

Figure 8. The spectral resolution of the interferometer is high enough to allow measurement of the response function in the presence of H_2O and CO_2 in the laboratory atmosphere.

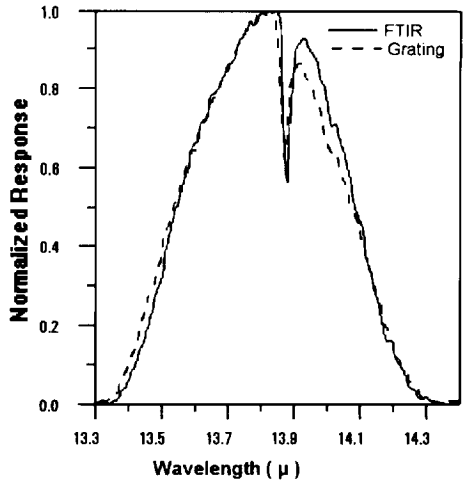

Figure 9. The spectral reporting accuracy of the two methods is evident in the CO_2 feature in channel 49.

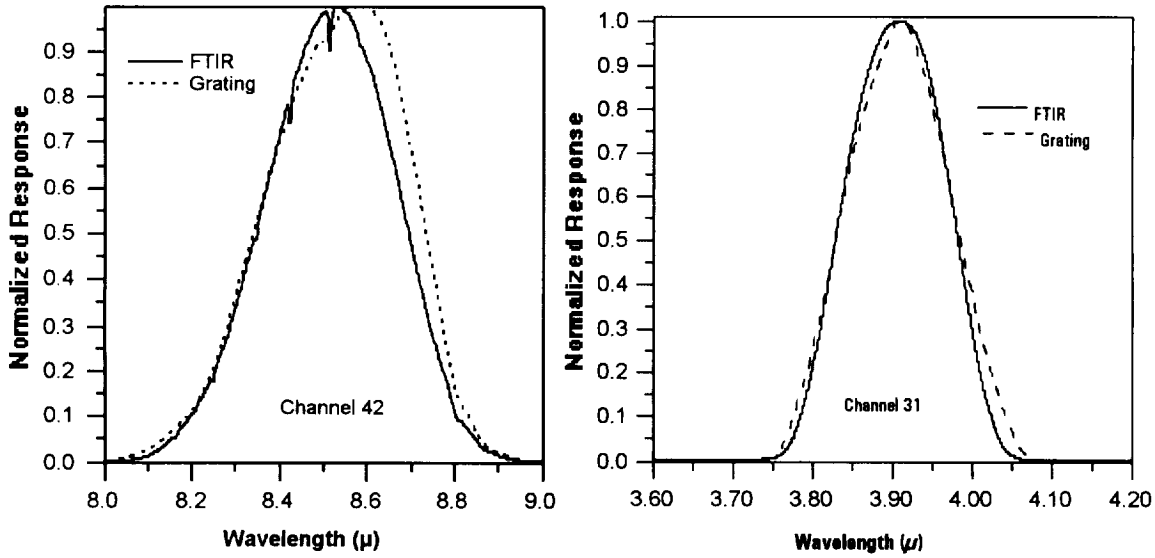

Figure 10. The comparison between the interferometer and grating calibration methods.

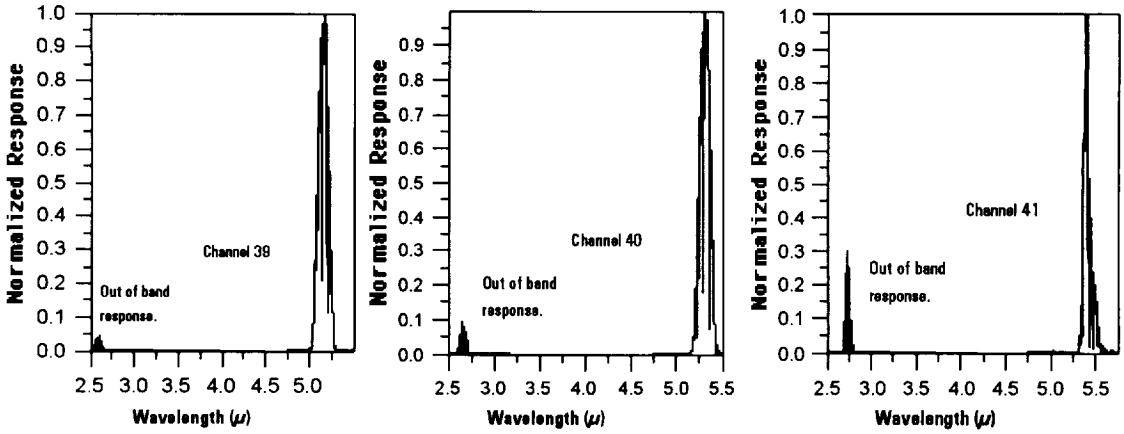

Figure 11. Out of band response discovered by the interferometer measurement system. Note : All data shown has been normalized but not corrected for the slope of the source radiance.

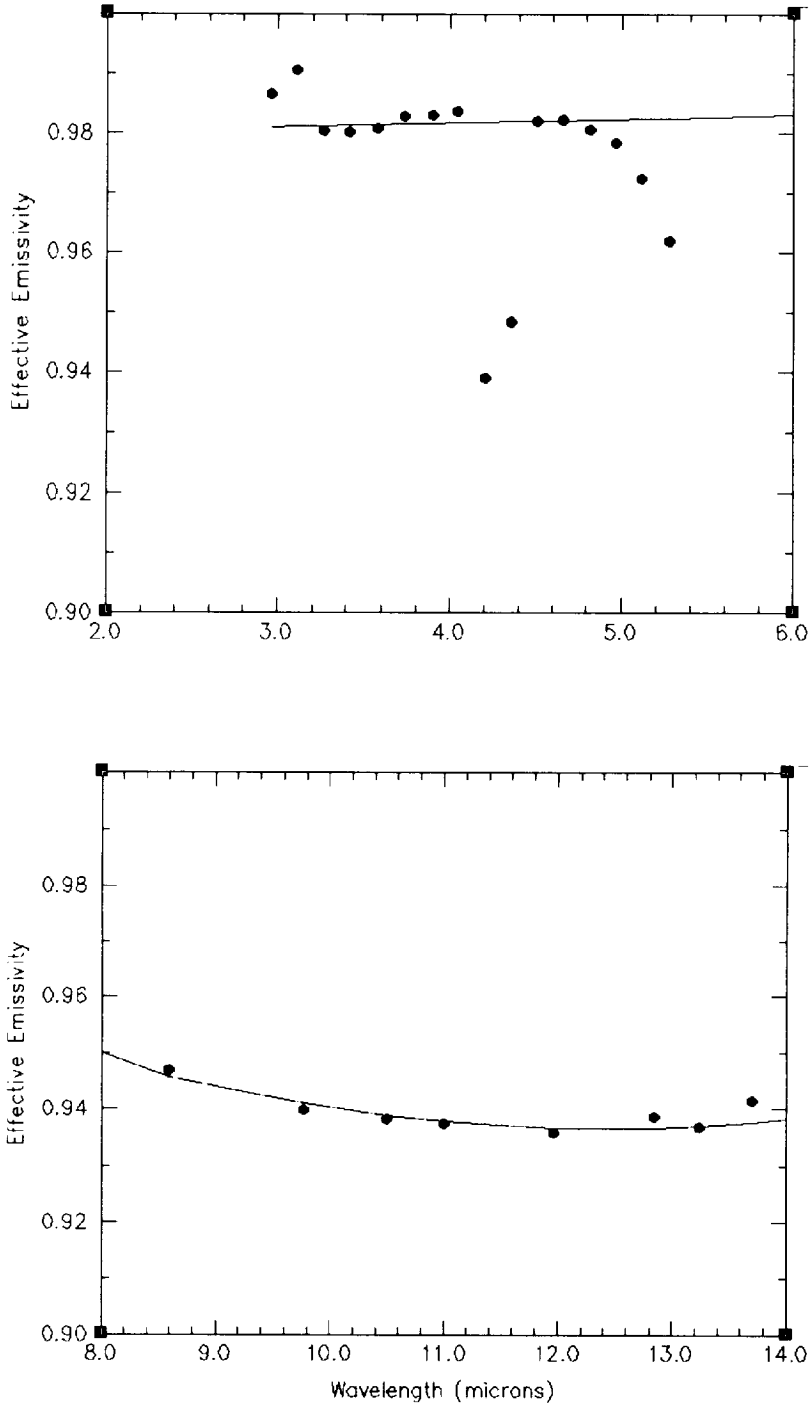

Figure 12. MAS onboard calibration blackbody effective emissivity estimates for SWIR (top) and LWIR (bottom). Selected data fit shown as solid line.

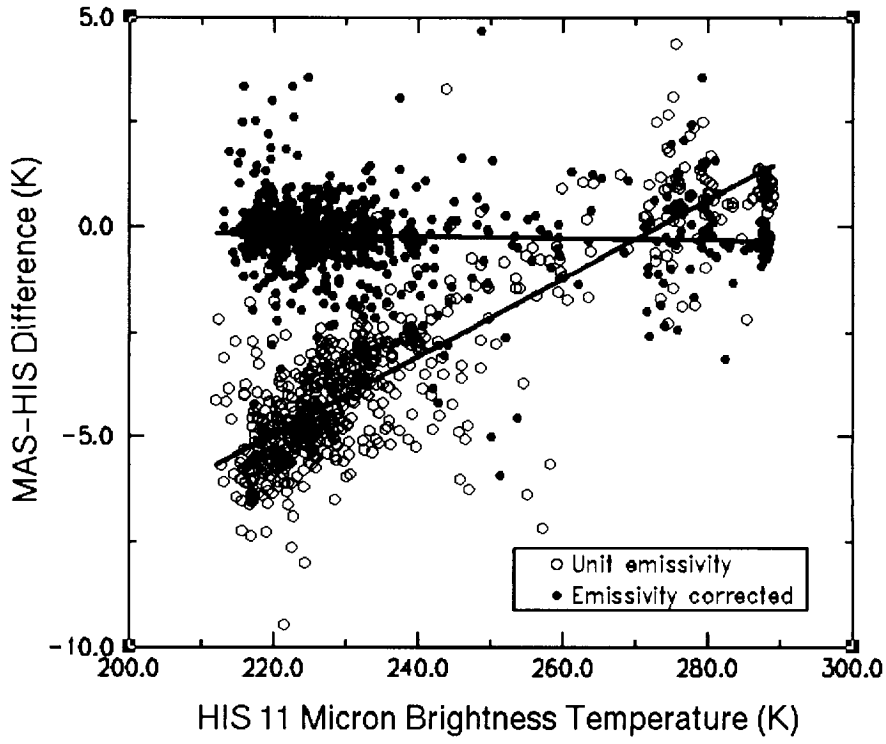

Figure 13. MAS-HIS 11μm brightness temperature bias as a function of scene temperature for MAS unit (open circles) and non-unit effective emissivity calibration (filled circles). Regression line for each is overlain. Using non-unit effective emissivity calibration almost entirely eliminates any bias dependence on scene temperature.